Characterization of stability, aggregation, and equilibrium properties of modified natural products; The case of carboxymethylated chitosans

Rilton Alves de Freitas [1] , Michael F. Drenski, Alina M. Alb, Wayne F. Reed *

Tulane Center for Polymer Reaction Monitoring and Characterization (PolyRMC), Tulane University, New Orleans, Louisiana, 70118, USA

ARTICLE INFO

ABSTRACT

Unstable biopolymer solutions inevitably lead to mis-characterization of macromolecular properties and irreproducible results. Even under stable or quasi-stable conditions, persistent aggregates can hamper reliable characterization, especially using light scattering methods. Various pitfalls in characterizing biopolymers were worked through, including determination of solution stability zones, dissolution kinetics, estimation of fraction of aggregate populations, and the relationship between batch and fractionation methods. Chitosans, polyampholytic biopolymers with isoelectric point around $pH = 6.0$, with varying degrees of carboxymethylation were studied. Instability was determined vs. pH and ionic strength using a high throughput screening method, simultaneous multiple sample light scattering (SMSLS). With stable solution conditions determined, equilibrium batch and multi-detector GPC characterization of molecular weight, intrinsic viscosity, and polyelectrolyte properties was made. Finally, a first attempt at continuous online monitoring of the modification reaction itself was made and compared to FTIR analysis of carboxymethylation on discrete aliquots. Given the range of possible characterization problems, multiple approaches with independent instruments may be required for reliable natural product characterization. Online monitoring of modification reactions may lead to rapid advances in understanding and preparation of natural products.

© 2009 Elsevier B.V. All rights reserved.

1. Introduction

Reliable characterization of biopolymers and their derivatives is a long standing challenge. Biopolymers, especially polysaccharides, are frequently unstable under many solution conditions, where aggregation is most often the mode of instability. Unstable biopolymer solutions inevitably lead to mis-characterization of macromolecular properties and irreproducible results. Even under stable or quasi-stable, small populations of persistent aggregates can continue to hamper reliable characterization and distort results.

The goal of this work is to confront issues of stability, effects of stable aggregates, and other problems to establish an experimental protocol for more reliably characterizing biopolymer solutions, modified chitosans in this case. First, regimes of solution physical stability under different pH and ionic strength (IS) conditions are rapidly assessed using a recently developed high throughput screening technique, simultaneous multiple sample light scattering (SMSLS), together with other characterization methods. Once the regimes of stability are established it is possible to deal with the problem of stable or quasi-stable aggregates and how they affect

characterization, especially when using light scattering methods. Another problem is the possible presence of significant fractions of oligosaccharides and other small molecules. This can lead to erroneous polymer concentrations used in batch measurement computations. Multi-detector gel permeation chromatography (GPC) can help resolve some of these problems and also be used to help correct batch measurements. Some authors refer to GPC as size exclusion chromatography (SEC) and when coupled to multi-angle light scattering (MALS), as SEC-MALS.

This study involves chitosans of varying carboxymethylation, which are polyampholytic macromolecules, with an isoelectric point around $pH = 6.0$. Use of natural biopolymers for diverse applications has advantages. Their use is ecologically sound and allows preparing chemically or enzymatically modified derivatives for specific uses. Polysaccharides tend to be bioactive, and are derived from agricultural feedstock or crustacean shell wastes. Cellulose, starch, pectin, etc. are derived from the former while chitin and chitosan are obtained from the latter. In terms of availability, chitin is next to cellulose, with over 10 Gt available annually [1,2].

Chitin and chitosan are linear copolymers of glucosamine with N-acetyl-glucosamine residues randomly distributed [2–4]. Characterization of chitosan by chromatographic methods is still inconclusive, and results reported are affected by aggregation, sample heterogeneity, and effects of acetylation on incremental refractive index, dn/dc

---

* Corresponding author.
[1] On leave from Pharmacy Dept., NIQFAR, Univali, Itajai, Brazil.

[5]. Brugnerotto et al. [6], using chitosan samples with various degrees of acetylation (DA) used SEC-MALS with a 0.3 M acetic acid/0.2 M sodium acetate diluent and obtained 95% sample recovery.

Carboxymethylchitosan (CM-chitosan) is the most fully explored chitosan derivative; it is an amphoteric polymer, with pH-dependent solubility. Under controlled reaction conditions (with sodium monochloracetate with NaOH), one obtains O- and N-carboxymethylation. Substituent yield on the three positions was determined by NMR [7,8]. This reaction extends the range of pH (pH > 7) in which chitosan is water-soluble, but a phase separation due to the balance between positive and negative charges on the polymer was observed at 2.5 < pH < 6.5.

Little characterization of CM-chitosan by SLS or multi-detector GPC exists, and there are still many ambiguities. Modification by carboxymethylation could decrease problems due to aggregation. Muzzarelli et al. [9] determined the molecular weight distributions (MWD) of carboxymethylated and sulfated chitosan using pullulan and dextrans as calibration standards. Chen et al. [10] determined MWD of O-carboxymethylchitosan with different degrees of acetylation. They also studied O-carboxymethylated chitosan by SEC-MALS, in 0.1 M NaCl. They observed heterogeneity in the samples, with a bimodal distribution [11]. Aiping et al. [12,13] studied aggregation of O-carboxymethylchitosan in neutral aqueous solutions. Dynamic light scattering (DLS) and atomic force microscopy (AFM) showed aggregate formation at low concentrations (0.05 mg/ml), increasing with ionic strength (IS), and with multivalent cations, Ca^{2+} and Cr^{3+}.

The preparation of N-carboxymethylchitosan (NCMC) by reaction with glyoxylic acid with a reducing agent is interesting due to mild condition of synthesis and in yield [5,11]. NCMC is soluble in water and also has unique chemical, physical and biological properties, low toxicity, biocompatibility, and film- or gel-forming capabilities, all of which make it attractive for use in food and cosmetics products [14,15]. Chemically, NCMC is a β-(1→4)-glucan, with 2-amino-2-desoxy-D-glucose and 2-carboxymethylamino-2-desoxy-D-glucose [13].

2. Materials and methods

2.1. Modified Chitosan samples

Chitosan was from Shangyu Biotech Co., Ltd (China, imported by Purifarma®, Brazil) and was produced from shrimp-shell chitin.

The N-carboxymethylation (CM) procedure was previously described [14,15]. To every 3.5 g of chitosan in 1 L of acetic acid (0.1 M, pH = 4.5), after 24 h of stirring, 50% glyoxylic acid solution was added to obtain derivatives with theoretical CM of 5, 25, 50, 75 and 100%, named respectively NCMC1, 2, 3, 4 and 5. The mixtures were kept under mechanical stirring for 24 h, the pH was adjusted to 8.0 with 0.1 M NaOH, and a 2% solution of $NaBH_4$ was added. The reaction was stirred an additional 24 h, pH was adjusted to 6–8, and the system filtered under vacuum. The filtered product (NCMC) was precipitated with 3 L of ethanol and dried at room temperature (25 °C) under vacuum.

Degree of chitosan deacetylation was assayed by Broussignac's method [16]. Chitosan was dissolved in 0.1 M HCl and titrated with 0.1 M NaOH. A curve with two inflexions points was obtained, and the difference of the volumes corresponds to the acid consumed for the salification of amine groups and allowed determination of DA. The degree of substitution of NCMC was evaluated by an alkalimetric curve, constructed by dissolving 0.25 g of NCMC, in 100 ml of water, bringing the solution to pH ~ 2 with 0.1 M HCl, and titrating with 0.1 M NaOH, or by the ratio of bands at 1540 and 3400 cm^{-1} [17,18]. A Thermo-Nicolet Nexus 670 FTIR was used.

^{13}C NMR spectra were obtained using a Bruker AVANCE-DRX-400. The solvent used was D_2O (Sigma-Aldrich), and NCMC samples were at 20 mg/cm^3 in salt form. The analysis was done at 70 °C. Chemical shifts at (δ) 179.1 and 52.0 ppm were attributed to carboxylic acid and N–CH_2, respectively, corresponding to carboxymethylation [18].

The chitosan used to synthesize NCMC derivatives showed a deacetylation degree of 87 ± 1.4%, determined by titration, and the intrinsic viscosity [η] and the viscosity-averaged molecular mass (M_v) were 450 cm^3/g and 0.92×10^5 g/mol, respectively, using 0.3 M acid acetic/0.2 M sodium acetate (pH 4.6) [19].

The anionicity is represented directly by the carboxymethylation of chitosan and the cationicity is a sum of the free amino groups not carboxymethylated and the weak base formed by the secondary amine during the carboxymethylation. The secondary amines have 1/10 of the cationicity of the primary group. The pKa of the anionic group was determined by titration to be approximately 4.4. The primary amino group pKa in chitosan is 6.5 [20].

2.2. Characterization instrumentation

A variety of methods were used for characterizing both batch (unfractionated) and fractionated sample properties. The batch quantities of chief interest included M_w, second virial coefficient A_2, z-average root mean square radius of gyration $R_{g,z}$ ($\equiv <S^2>_z^{1/2}$), weight average intrinsic viscosity $[\eta]_w$, solute concentrations, and z-average diffusion coefficient D_z. In some cases the time dependence of such properties was also measured. Multi-detector GPC was used as a fractionating characterization method.

For SLS measurements, analysis was according to Zimm's method [21], using 7 angles, nominally 35, 50, 75, 90, 105, 130 and 145°, at concentration of 1 mg/mL, whose equation at low concentrations and for $q^2<S^2>_z \ll 1$, is

$$\frac{Kc}{I_R(q,c)} = \frac{1}{M_w}\left(1 + \frac{q^2\langle S^2\rangle_z}{3}\right) + 2A_2c \qquad (1)$$

where $I_R(q,c)$ is the excess Rayleigh scattering ratio (cm^{-1}) at scattering vector q and polymer concentration c (g/cm^3). K is an optical constant, given for vertically polarized incident light by

$$K = \frac{4\pi^2 n^2 (dn/dc)^2}{N_A \lambda^4} \qquad (2)$$

where n is the solvent index of refraction, λ is the vacuum wavelength of the incident light, dn/dc is the differential refractive index for the polymer in the chosen solvent, and $q = (4\pi n/\lambda)\sin(\theta/2)$, where θ is the scattering angle. Eq. (1) permits direct determination of M_w, A_2 and the z-averaged mean square radius of gyration $<S^2>_z$. The dn/dc was determinate using a Waters RI detector calibrated using NaCl. The sample concentration was from 0.1 to 1 mg/mL using water.

2.2.1. Solution stability was monitored using simultaneous multiple sample light scattering (SMSLS)

The custom-built SMSLS system has been described [22,23]. SMSLS allowed monitoring the light scattered at 90° for several samples simultaneously, in static cells and/or flow cells.

2.2.2. Automatic continuous mixing (ACM) allowed assessment of batch characteristics

The custom built ACM has been described [24,25]. It is well suited for determining M_w, A_2, $R_{g,z}$, solute concentrations, and $[\eta]_w$ in multi-component solutions by automatically creating programmable solute concentration gradients. Here, two types of gradients were used; 1) ramping NCMC concentration at fixed IS (generally 0.1 M aqueous NaCl) and 2) ramping IS from 0 to 0.1 M at fixed NCMC concentration (generally 0.001 g/cm^3). The system used a Shimadzu LC-20AT and Shimadzu quaternary mixing module FCV13AL, a Brookhaven BI-MwA multi-angle light scattering detector (MALS), a Waters RI detector, and a custom-built single capillary viscometer [26].

2.2.3. ACM in recirculation mode was used to measure dry polymer dissolution kinetics

As a prelude to determining stability regimes and other solution characteristics the dissolution kinetics of samples was measured using the recirculation method of Michel and Reed [27]. The recirculation flow rate was 1 ml/min and the response time was 40 s, determined by injection of 0.1 M NaCl solution into the dissolution reservoir.

2.2.4. Dynamic light scattering (DLS)

A Brookhaven instruments BI-90 plus, with 90° detection was used for intensity autocorrelation computation and analysis by the standard method of moments [28] to yield average D_z and the higher moments. From D_z the z-averaged equivalent sphere hydrodynamic radius R_H was determined by the Stokes–Einstein relationship for spheres. Because the measured quantity is a z-average of the population, the measurement is very susceptible to small populations of aggregates.

2.2.5. Multi-detector gel permeation chromatography (GPC)

Principles and specifics of multi-detector GPC have been reviewed [29]. The system used here comprised a Shimadzu LC-20AT pump, Brookhaven Instruments Corp. BI-MwA MALS detector, a Waters RI, and a custom-built viscometer.

3. Results

3.1. Initial results of monitoring the NCMC synthesis reaction

Chitosan at 3.5 mg/ml was dissolved in acetate buffer (0.1 M) at pH = 4.5 and reacted with 1.44 g/L of glyoxylic acid ([chitosan]/[glyoxylic acid = 1). A recirculation loop from the reactor through the detector train allowed continuous reaction monitoring by MALS, viscosity and conductance. M_w and $\eta_{r,w}$ vs. t are shown in Fig. 1a. (In this work concentrations are low enough to consider $\eta_{r,w} \cong [\eta]_w$). Additionally, aliquots were removed during the reaction for FTIR analysis of carboxymethylation. For this, the imine group was reduced with NaBH$_4$, the pH adjusted to 7.4, and the samples precipitated with ethanol.

Fig. 1a shows that viscosity decreased and conductance increased. M_w remained constant, indicating there was no significant degradation or cleavage of the chitosan backbone. The viscosity decrease is likely due to the increasingly polyampholytic nature of the polymer as carboxylate groups form, and polymer size begins to decrease. R_H by DLS was 110 nm at $t = 0$, and fell to 74 nm after 48 h.

The degree of carboxymethylation determined by FTIR is shown in Fig. 1b, with sample spectra in the inset. Also, at 1740 cm^{-1} it was possible to observe an increase of the absorption related to carboxylic acid groups, confirming the modification. The first order kinetic fit to the carboxymethylation data from FTIR yielded 1.75×10^{-3} min^{-1} and is shown in Fig. 1b.

The first attempt at correlating the continuous viscosity and conductivity data with the % carboxymethylation obtained by the first order fit to the data derived from the offline FTIR spectra. There are strong correlations of each quantity – e.g. viscosity drops most strongly after 50% carboxymethylation, but there is no descriptive model for their interpretation at this point (data not shown). The monitoring approach is left here as a starting point to possible important advances in the area that will allow for monitoring and controlling natural product modification reactions.

3.2. Dissolution kinetics

Dry polymers, especially high molecular weight polysaccharides, can take considerable time to dissolve. For both the sake of efficiency and quality of solutions for subsequent characterization and use, it is
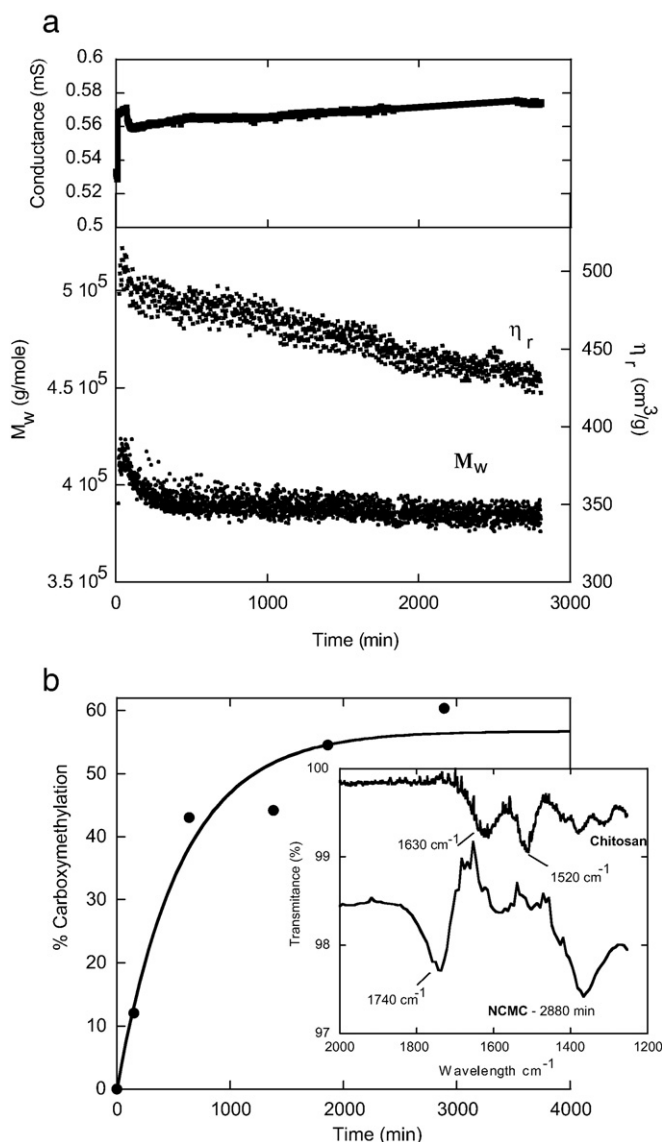
Fig. 1. a. Continuous monitoring of chitosan carboxymethylation by light scattering, LS90°, viscosity and conductance. b. % carboxymethylation from FTIR data on aliquots. Inset shows examples of FTIR spectra used.

valuable to have a quantitative means of determining dissolution kinetics.

Dissolution kinetics were measured by the recirculation method, dissolving dry polymer samples in water at 25 °C and pH 9 at which the carboxymethyl groups of NCMC are 100% ionized. Samples included NCMC with different degrees of carboxymethylation: 23.5, 63 and 83.6%, respectively NCMC2, NCMC4 and NCMC5. Fig. 2 shows the results. The % dissolution was determined from the RI signal, whose increase quantitatively measures the amount of dissolved polymer mass. An inline frit filter of 2 μm was used in the recirculation loop.

Fig. 2 shows that all samples start to dissolve at 200 s whereas NCMC2, with lower carboxymethylation dissolved more slowly (2000 s). The solid lines in Fig. 2 are first order (exponential) fits, whose rates vary systematically with the % of carboxymethylation; 0.0087 s^{-1}, 0.0091 s^{-1} and 0.012 s^{-1} for NCMC2, NCMC4 and NCMC5, respectively. The powder of NCMCs samples showed approximately the same diameter (< 125 μm), as previously obtained by sieving.

dn/dc was determined during these experiments to be 0.120 +/− 0.004 cm^3/g for NCMC2 and NCMC4, assuming that 100% dissolution
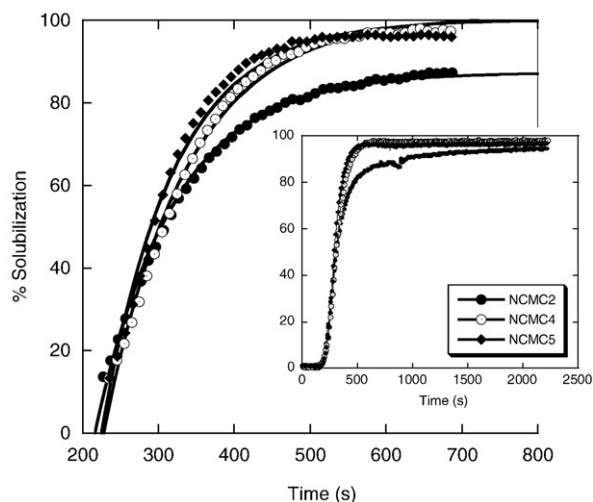
Fig. 2. Carboxymethylation effects on dissolution of NCMC2 (23.5%), NCMC4 (63%) and NCMC5 (83% of carboxymethylation), with first order fits. Inset shows longer term behavior.

occurred on the RI signal plateau. This value was used in subsequent determinations of concentration loss by filtration and in MALS analysis. The value is in good agreement with literature values for O-carboxymethylchitosan with similar degree of carboxymethylation and deacetylation (0.126 cm^3/g) [15].

3.3. Determining regimes of stability for solutions

In some cases it was obvious that dry samples will not dissolve completely in a given solvent; e.g. in 0.1 M Tris buffer with 0.1 M NaCl. In other cases, stability was determined first by dissolving the sample in pure water, or in aqueous 0.010 M or 0.1 M NaCl, and then adding HCl or NaOH to adjust the pH. SMSLS was used to investigate stability for up to 48 h. In the case of precipitation, the SMSLS signals would fall abruptly, since the precipitating particles would fall below the incident laser beam in the sample cells. In general, concentrations of NaCl up to 0.1 M alone did not have a large effect on stability.

The SMSLS signals would either remain constant (up to 48 h) — indicating a stable or quasi-stable solution, or decrease — indicating that the material, including aggregates is still dissolving, or increase — demonstrating that aggregates are forming. Stability was cross-checked by DLS. When instabilities occurred R_H would also increase or decrease accordingly. 'Quasi-stable' here means that there is no detectable change due to aggregation or precipitation in solution during a period of time much longer than that needed for preparation and measurement of a given solution; i.e. 48 h is at least quasi-stable by this definition.

The reversibility of the precipitation and aggregation was confirmed by adding NaOH to acidified solutions, and verifying that the material re-dissolved immediately.

Fig. 3 shows several stability profiles of NCMC2 and NCMC4, during 24 h of the complete 48 h analysis. The scattering data is represented as $I_R/Kc(90°)$, which is a rough measure of M_w (i.e. the $θ = 90°$ value). Sample stability was observed at most pH values, except around pH = 8, where measurable, time-dependent aggregation took place. The R_H by DLS also increased proportionally, for NCMC2 from 220 to 240 nm, and for NCMC4 from 84 to 112 nm, over the monitored aggregation period. The slow decrease in I_R/Kc for NCMC2 at pH 5 and 7 is attributed to slow dissolution of residual aggregates before reaching a stable plateau.

The nature of the stable or quasi-stable aggregates was further explored using MALS in a flow cell, with pre-filtration through a 0.22 μm membrane filter and a 2 μm inline filter (data not shown).
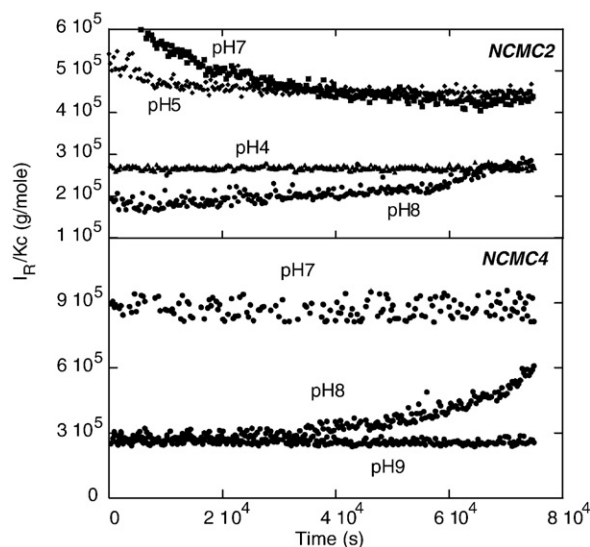
Fig. 3. Stability tests, using SMSLS, of the samples NCMC2 and NCMC4, at 1 mg/mL in water, after filtration by 0.22 μm, 25 °C.

These confirmed the SMSLS results, and showed highly angular dependent I_R, indicating large particles.

3.4. Effects of different types of solution filtration on stable or quasi-stable aggregates

After determining dissolution kinetics and stable solution conditions, the next step was to identify the best filtration system for the NCMC samples, to assess the presence of aggregates. Fig. 4 shows the effect of filtration on NCMC2 by monitoring the RI, MALS, and viscosity detectors as the solubilized sample flowed through them. The RI signals allowed concentrations to be computed and thus the loss of material by filtration to be evaluated using 0.8, 0.45 and 0.22 μm filters. As seen in Fig. 4 there is very little change in RI signal, and there was at most a 5% loss of material during 0.22 μm filtration.

In contrast, filtration has a dramatic effect on LS intensity. LS intensity is due to both isolated macromolecules and aggregates, and
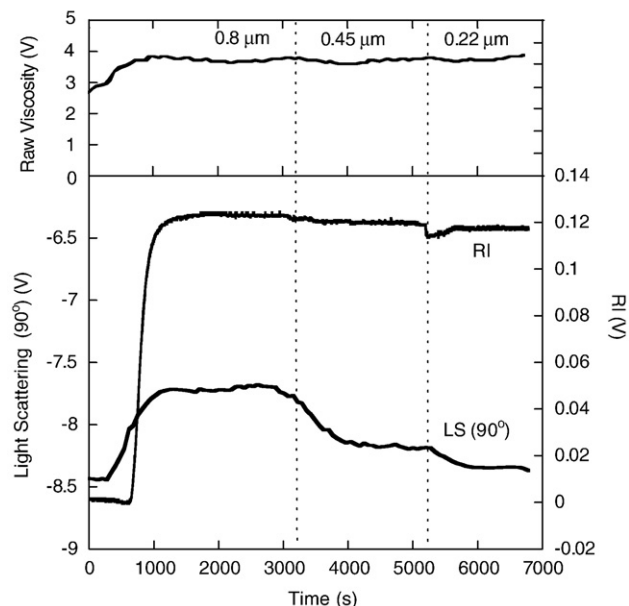
Fig. 4. Effect of filtration on NCMC2 in water, pH 9, as monitored by raw viscosity, LS90°, and RI.

clearly, removing a small mass fraction of the population has a much larger effect on LS than on the concentration-measuring RI signal. The upwards curvature of the Kc/I_R vs. q^2 data in Fig. 5 for samples filtered by 0.45 and 0.8 μm is a classical hallmark of spheroidal scatterers, such as microgels [30]. In contrast, the downwards curvature seen for the sample filtered through 0.22 μm is characteristic of very massive, highly polydisperse coil polymers. These data show the importance of filtration as concerns LS measurements. Because LS measures M_w, small populations of aggregates and/or microgels can dominate the LS and distort the interpretation. Even at 0.22 μm filtration, the scatterers are more massive and larger in size than for the Kc/I_R GPC elution slice data also shown, which is a straight line with a relatively small slope.

The interpretation that a small population of aggregates is removed by filtration is confirmed by the viscosity data in Fig. 4. The viscosity was practically independent of filtration, with a maximal reduction of 3.4%, suggesting the removal of aggregates that have low $[\eta]_w$ and hence contribute almost nothing to total solution viscosity. $[\eta]_w$ for aggregates is low because $[\eta]$ is proportional to hydrodynamic volume per unit molecular weight, and spheroidal aggregates and densely overlapping coils (Fig. 5) yield structures with low volume per mass.

3.5. Equilibrium characterization

Having established the pH 9.0 and IS zones of stability, and understanding better the effects of filtration, it was possible to proceed to equilibrium characterization of the NCMC.

3.6. ACM

In the first ACM measurements, polymer concentration was ramped from 0 to a nominal 0.001 g/cm^3 in aqueous 0.1 M NaCl at pH = 9. Corrected concentrations were determined from GPC results, discussed below. Fig. 6 shows LS90^0 and weight average specific viscosity, $\eta_{sp,w} = c\eta_{r,w}$ (i.e. $\eta_{sp,w}$ = fractional increase in solvent viscosity due to the presence of the polymer) vs. c for NCMC2. The polymers were filtered sequentially through 0.8, 0.45 and 0.22 μm membrane filters before the ACM ramp. The values of M_w, A_2 and $[\eta]_w$ are shown in Table 1. In this table and in Figs. 6 and 7, GPC-corrected concentrations were used.

Whereas the modification monitoring experiment (Fig. 1a–b) showed no significant change in M_w during the reaction, there is nonetheless a significant M_w decrease between the NCMC2 and NCMC4 prepared previously by modification and recovered separate-
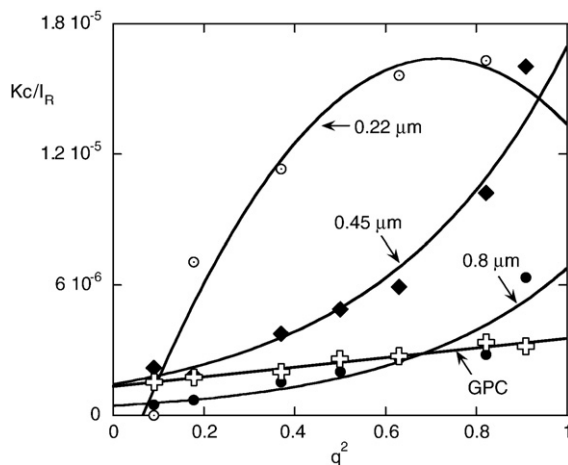
Fig. 6. Light scattering (90°), and specific viscosity vs. polymer concentration in NaCl 0.1 M.

ly by precipitation. The differences between the different pre-prepared samples might be due to the precipitation process after glyoxylation and reduction with NaBH$_4$, with different fractions of polymers precipitating with 2 volumes of ethanol, resulting in differences in M_w.

Fig. 7 shows raw LS90° and $\eta_{r,w}$ for NCMC2 at nominal 0.001 g/cm^3 at pH 9, under an NaCl ramp from 0 to 0.1 M. The behavior is typical of polyelectrolytes. Namely, as IS increases the charges on the polymer chain are increasingly shielded electrostatically, allowing the polymer coil to contract. This both lowers the viscosity, as seen by the dramatic decrease, and increases LS, since A_2, which is largely electrostatic in origin at low IS, decreases.

3.7. Multi-detector GPC

It might be thought that GPC could resolve the issues of aggregates, multi-modal populations, and other effects, that cannot be separated by batch measurements alone. The following results demonstrate, however, that GPC is also fraught with its own difficulties.

Two different GPC eluents were used: #1) aqueous 0.1 M Tris with 0.1 M NaCl at pH = 9, in the stable aggregate zones for NCMC2 and NCMC4. #2) aqueous 0.1 M sodium acetate/acetic acid at pH 6. Injected solutions were pre-filtered through a 0.22 μm membrane filter.

Fig. 8 shows raw chromatograms for RI and LS90 for NCMC2 with eluents #1 and #2. In eluent #1 there is a strong LS peak associated with the RI peak at low elution volume, e.v. = 15.14 mL. This corresponds to the polymeric fraction and constitutes 48% of the injected material. In eluent #2 there is neither an RI nor LS signal at

Fig. 5. Inverse scattering envelopes for stable aggregates filtered through different membrane pore sizes, from the NCMC2 data of this figure. Also shown are data points from a typical GPC elution slice of NCMC2.

Table 1
ACM results for NCMC2 and NCMC4.

	NCMC2	NCMC4	How L'_p was computed	
			L from	$\langle S^2\rangle^{1/2}$ from
M_w	1.05×10^6	4×10^5		
$R_{g,z}$ (Å)	1220	1320		
$[\eta]_w$ (cm^3/g)	215	191		
$R_{\eta,w}$ (Å)	440	273		
A_2 (cm^3 mol/g^2)	3.56×10^{-3}	2.2×10^{-3}		
R_{eq} (Å)	752	318		
R_H (Å)[a]	670	680		
$L_{p,w,z}$ (Å)	162	584	M_w	$R_{g,z}$
$L_{p,\eta,w}$ (Å)	17	24	M_w	R_η from$[\eta]_w$
$L_{p,A2,w}$ (Å)	60	33	M_w	R_{eq}
$L_{p,RH}$ (Å)	48	152	M_w	R_H

[a] From batch DLS measurements.
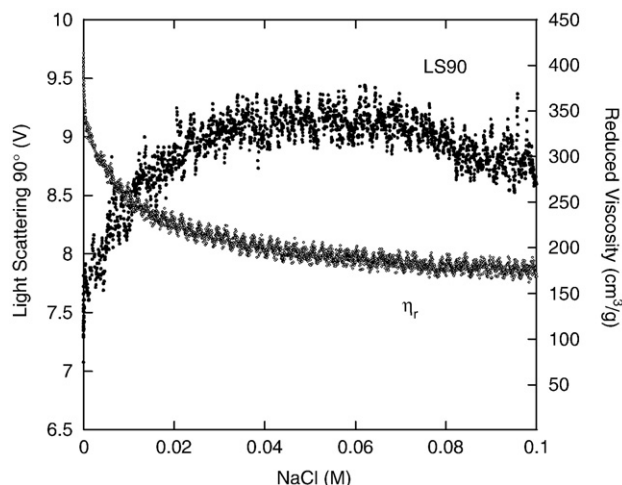
Fig. 7. Light scattering (90°) and reduced viscosity vs. NaCl, for a solution of 0.00048 g/cm³ NCMC2.

the low e.v., but there is a considerable RI signal, with no corresponding LS at higher e.v. = 20.7 mL, which corresponds to 41% of the injected material. These estimates of eluted material assume the same dn/dc (=0.120) for both fractions. They are obtained by integrating the RI peak over e.v. to obtain total mass eluted, and comparing this with the known, injected mass, computed by $c_{inj}V_{inj}$, where c_{inj} is the concentration of the injected sample, and V_{inj} the injection loop volume (100 µl in this case).

It is important to note that the chromatogram for the parent chitosan, from which the derivative NCMC series were obtained by modification, also showed the low mass fraction of material at the higher e.v. (data not shown).

The aggregates are excluded as can be seen by the linearity of the Kc/I vs. q^2 data for GPC (volume 13.5 ml) in Fig. 5, which contrasts sharply with the highly sloped and curved data of the aggregates measured in batch. Thus, in the case where elution of the polymeric portion is obtained, the aggregates are excluded.

Furthermore, the GPC data show that the weighed sample concentration is not all in polymeric form. As concerns the fraction of low mass material measured in eluent #2, its identity cannot be stated without further chemical analysis. It may be composed largely of oligosaccharide fragments that are already in the parent chitosan, and are perhaps a result of the deacetylation treatment of the original chitin. These oligosaccharides may co-precipitate with the chitosan
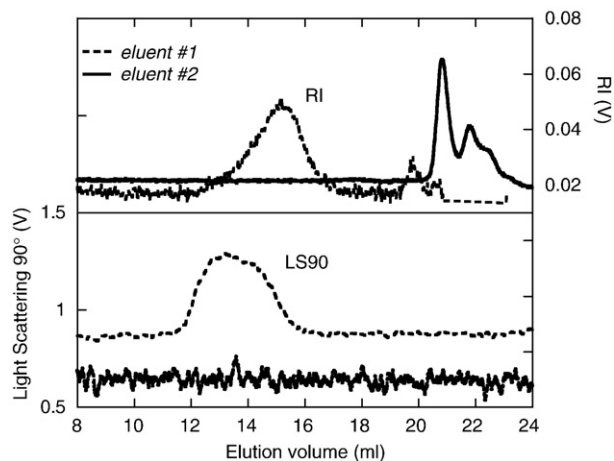
Fig. 8. Raw chromatograms of GPC for RI and LS90° profile for NCMC2 with eluents #1) aqueous 0.1 M Tris with 0.1 M NaCl at pH = 9 and #2) aqueous 0.1 M sodium acetate/acetic acid at pH 6.

derivatives during ethanolic precipitation. It will be possible to identify the chemical nature of the low mass fraction in future work using NMR, mass spectrometry, and total sugar assays.

The GPC determination of the fraction of polymeric content in the NCMC samples was used to correct the concentrations used in batch measurement computations. GPC determined polymeric contents of 48% and 14% for NCMC2 and NCMC4. These corrected concentrations to the weighed values were used in Fig. 7a,b, and in the values for M_w, and $[\eta]_w$ shown in Table 1. It is important to point out that determination of R_g and A_2 are *independent* of polymer concentration.

Using eluent #1 permitted GPC characterization of the samples' polymeric portion. Table 2 summarizes various averages for molecular weight, R_g and $[\eta]$ obtained from the GPC results. Interestingly, column calibration by PEO standards led to values fairly close to those yielded by GPC-MALS (see $M_{peak,peo}$ in Table 2).

3.8. Comparison of different equilibrium approaches; focus on sizing and apparent persistence length

For both NCMC2 and NCMC4 M_w, as measured by ACM, is significantly higher than the corresponding value of M_w from GPC, seen by comparing Tables 1 and 2. This is because GPC columns tend to block, and in some instances also degrade aggregates and large chains, and there can also be selective adsorption of cationic polymers on the column. Fig. 5 shows Kc/I_R vs. q^2 plot of a typical GPC elution slice is a straight line, much different from the highly curved plots obtained for batch measurements on samples filtered through different pore sizes; i.e. the very nature of the high mass material eluting from GPC is much less dense and spatially extended than the aggregates found in batch measurements, and that even after 0.22 µm filtration batch SLS still measures aggregates.

There is better agreement between $[\eta]_w$ computed by ACM and GPC, because $[\eta]_w$ is much less sensitive to aggregates than light scattering, as discussed above. This again re-enforces the use of viscosity measurements as a means of confronting the problem of aggregates.

Persistence length L_p, is a useful concept for gauging polymer stiffness. In the wormlike chain model it is related to polymer contour

Table 2
GPC and L'_p results for NCMC2 and NCMC4.

	NCMC2	NCMC4	Definition of L'_p	
			L from	$<S^2>^{1/2}$ from
% polymer elution	48	14		
M_n	80,300	39,600		
M_{peak}	102,000	36,300		
$M_{peak, peo}$[a]	110,000	42,400		
M_w	395,000	188,000		
M_z	2.16×10^6	1.7×10^6		
M_w/M_n	4.92	4.75		
M_z/M_w	5.45	9.11		
$R_{g,w}$ (Å)	840	380		
$R_{g,z}$ (Å)	1090	830		
$[\eta]_w$ (cm³/g)	280	180		
$R_{\eta,w}$ (Å)	307	208		
$R_{\eta,w,z}$ (Å)	540	430		
$L_{p,w}$ (Å)	202	99	M_w	$R_{g,w}$
$L_{p,z}$ (Å)	62	53	M_z	$R_{g,z}$
$L_{p,\eta,w}$ (Å)	27	30	M_w	$[\eta]_w$
$L_{pRg,p-p}$	135	69	M each elution point	R_g at each elution point
$L_{p,\eta,p-p}$	35	37	M at each elution point	R_η at each elution point

$L_{p,w,z} = M_w$ and Rg_z.
$L_{pRg,p-p} = L_p$ averaged over individual $L_{p,i}$ from chromatogram from Rg.
$L_{p,\eta,p-p} = L_p$ averaged over individual $L_{p,i}$ from chromatogram from viscosity.
[a] M_{peak} determined by PEO standards.

length L and unperturbed mean square radius of gyration $<S^2>_0$, which is the value in Θ-solvent conditions (no excluded volume)[30];

$$\langle S^2 \rangle_0 = \frac{L L_p}{3} - L_p^2 + 2L_p^3/L - 2\left(\frac{L_p^4}{L^2}\right)[1 - \exp(-L/L_p)] \qquad (3)$$

In reality, scattering measures the perturbed $<S^2>$, consisting of $<S^2>_0$ and intrachain excluded volume. It is seldom possible experimentally to separate intrinsic stiffness from excluded volume directly, so the two effects together can be conveniently assessed via the 'apparent persistence length', L'_p [31]. The measured $<S^2>$ is often related to $<S^2>_0$ by the static expansion factor α_s; $<S^2> = \alpha_s^2 <S^2>_0$, where α_s includes excluded volume. $<S^2>_0$ can be replaced by $<S^2>$ in Eq. (3), and the 'apparent persistence length', L'_p, is obtained which is a nearly mass-independent measure of coil 'expansivity'. L'_p is robust in this sense since it varies weakly with M, at a maximum as $M^{0.2}$. This latter assertion is a consequence of the experimental and theoretical limits of the scaling coefficient β in $<S^2>^{1/2} = bM^\beta$ falling in the range of 0.583–0.600 for coil molecules.

The presence of aggregates, of course, calls into question the whole use of the persistence length notion.

Other authors working with chitosan have extracted 'true' (unperturbed) rather than 'apparent' persistence lengths by making model-dependent computations of excluded volume via α_s or equivalent, and have found values averaging 50 Å[6], and in the range of 100–150 Å [7].

Tables 1 and 2 give the values of L'_p represented in several ways, to illustrate both the various approaches to its computation, and the effects of using different averages of the characteristic distributions. L'_p measurements are shown using $R_{g,z}$ from MALS, R_{eq} from A_2, and $R\eta$ from $[\eta]_w$. Traditionally, the measurements are based solely on light scattering measures of $<S^2>$, but here the results of other sizing approaches are shown.

L was computed from molecular weight with the following conversions: NCMC2 = 206 (g/mol)/5.5 Å = 37.5 g/(mol Å), and NCMC4 = 242 (g/mol)/5.5 Å = 44 g/(mol Å).

The effective viscometric radius $R\eta$ can be found by starting with Flory's equation for $[\eta]$ of chains in Θ-solvents in the non-draining limit, $[\eta]_0$; In terms of $<S^2>_0$,

$$[\eta]_0 = 6^{3/2} \frac{\Phi}{M} \langle S^2 \rangle_0^{3/2} \qquad (4)$$

where $\Phi = 2.56 \times 10^{23} \, mol^{-1}$. Flory and Fox [32] proposed using Eq. (4) with the measured, good solvent value $[\eta]$ and hence the perturbed values of $<S^2>_0$; i.e. $<S^2>$. They introduced the viscosity expansion factor $\alpha\eta$, relating the good solvent to Θ-solvent viscosities via $[\eta] = \alpha_\eta^3 [\eta]_0$. Extensive work on deriving expressions for $\alpha\eta$ has been carried out [33–35]. Here, the effective viscometric radius $R\eta$ is defined according to the experimentally measured values of $[\eta]_w$ and M_w by

$$[\eta]_w = 6^{3/2} \frac{\Phi}{M_w} R_\eta^3 \qquad (5)$$

Separately, the equivalent excluded volume radius R_{eq} can be obtained from the ACM A_2 data by

$$A_2 = \frac{N_A}{2M^2} \frac{32\pi R_{eq}^3}{3} \qquad (6)$$

Table 1 shows the expected result that equivalent radii computed from light scattering quantities of MALS and DLS are higher than the viscosity derived $R\eta$, reflecting the fact that light scattering measures higher moments of these very polydisperse samples.

The various L'_p defined in Tables 1 and 2 are shown in the fourth column of each. There is extremely wide variation in the values

obtained, and this reflects the presence of aggregates and combining very different moments of the mass distribution in batch measurements, as well as the different properties used to compute '$<S^2>$' in Eq. (3). In general, viscosity based determinations of L'_p are less than the light scattering based determinations. Averaging over the various values yielded: NCMC2 $L'_p = 73$ Å $+/-$ 22 Å, and NCMC4 $L'_p = 63$ Å $+/-$ 32 Å. These values are in the range noted above for chitosan. At any rate, they represent a semi-flexible polymer a bit on the low side for single stranded polysaccharides, but substantially higher than most synthetic polymers; synthetic polymers typically have $L'_p \sim 10$ Å, single chain polysaccharides with significant helical structure typically are on the order of 100 Å (e.g. hyaluronans), and double-stranded polymers are typically much stiffer with $L'_p \sim 1000$ Å (e.g. xanthans).

4. Conclusions

A series of experimental methods are elaborated for dealing with complex, aggregating biopolymer solutions. It has been demonstrated that carboxymehtylated chitosans are highly prone to aggregation in solution, and that only certain ranges of solution conditions, such as pH and ionic strength, lead to stable or quasi-stable solutions. Only in stable zones can meaningful equilibrium characterization of the biopolymers be made. Irreproducible results will result when working, wittingly or not, in unstable zones. Even in stable solutions, there can be persistent aggregates which make up a small mass fraction of the population (less than 5% here). This can make meaningful light scattering experiments difficult, unless the small population of aggregates is removed. Otherwise, light scattering will be dominated by the aggregates. Proper filtration and cross-checks between batch light scattering and GPC-based light scattering can help establish the conditions for minimizing the effects of aggregates. The aggregates themselves can be present as microgels (upwards curvature in Kc/I vs. q^2) or as massive, highly polydisperse aggregates of random coils (negative curvature of Kc/I vs. q^2). Because of the seriousness of the aggregate problem, it is useful to make viscosity measurements, since these are virtually unaffected by small populations of aggregates. It is nonetheless vitally important in the viscosity measurements to have good estimates of the amount of polymeric material in a sample, since including oligomeric and small molecule mass in the concentration can seriously distort values of $[\eta]$.

SMSLS, ACM, and DLS have all proved useful for mapping out the stable zones for the biopolymer solutions. SMSLS is particularly well adapted for high throughput determinations of aggregating and non-aggregating zones, since many samples can be measured and screened simultaneously. Once stable zones are identified and aggregates minimized, the polymeric characteristics of the materials can be found.

A significant first step in this work was taken in real-time monitoring of the modification reactions that produce chitosan derivatives. These demonstrated no degradation of the chitosan. Correlations between the continuously monitored conductance and viscosity with % carboxymethylation were found but are not interpreted within a descriptive model at this point. Further development and refinement of this online method could be extremely valuable for accurately and quantitatively controlling natural product modifications.

References

[1] K. Kurita, Prog. Polym. Sci. 26 (2001) 1921.
[2] K.V.H. Prashanth, R.N. Tharanathan, Trends Food Sci. Technol. 18 (2007) 117.
[3] C. Chatelet, O. Damour, A. Domard, Biomaterials 22 (2001) 261.
[4] R.A.A. Muzzarelli, Chitin, Pergamon, Oxford, 1977, p. 105.
[5] C. Schatz, C. Viton, T. Delair, C. Pichot, A. Domard, Biomacromol. 4 (2003) 641.
[6] J. Brugnerotto, J. Desbrières, G. Roberts, M. Rinaudo, Polymer 42 (2001) 9921.
[7] M. Rinaudo, P. Le Dung, C. Gey, M. Milas, Int. J. Biol. Macromol. 14 (1992) 122.
[8] P. Le Dung, M. Milas, M. Rinaudo, J. Desbrières, Carbohydr. Polym. 24 (1994) 209.
[9] R.A.A. Muzzarelli, F. Tonfani, M. Emanuelli, S. Mariotti, Carbohydr. Res. 107 (1982) 199.
[10] L. Chen, Y. Du, X. Zeng, Carbohydr. Res. 338 (2003) 333.
[11] L. Chen, Y. Du, T. Zhigang, L. Sun, J. Polym. Sci. 43 (2005) 296.
[12] Z. Aiping, M.B. Chan-Park, D. Sheng, L. Lin, Colloids Surf. B 43 (2005) 143.
[13] Z. Aiping, D. Sheng, L. Lin, Z. Feng, Colloids Surf. B 47 (2006) 20.
[14] M.E.S. Miranda, C. Marcolla, C.A. Rodrigues, H.M. Wilhelm, M.R. Sierakowski, T.M.B. Bresolin, R.A. Freitas, Polym. Int. 55 (2006) 961.
[15] R. Lamim, R.A. Freitas, E.I. Rudek, H.M. Wilhelm, O.A. Cavalcanti, T.M.B. Bresolin, Polmy. Int. 55 (2006) 970.
[16] P. Broussignac, Chim. Ind. Gén. Chim. 99 (1968) 1241.
[17] G. Di Colo, Y. Zambito, S. Burgalassi, I. Nardini, M.F. Saettone, Int. J. Pharm. 273 (2004) 37.
[18] H.C. Ge, D.K. Luo, Carbohydr. Res. 340 (2005) 1351.
[19] M. Rinaudo, A. Domard, in: P. Sandford (Ed.), Solution properties of chitosan, Chitin and Chitosan: Sources, Chemistry, Biochemistry, Physical Properties and Applications, Elsevier Applied Science, London, 1989, p. 71.
[20] L. Chen, Z. Tian, Y. Du, Biomaterials 25 (2004) 3725.
[21] B.H. Zimm, J. Chem. Phys. 16 (1948) 1093.
[22] M.F. Drenski, W.F. Reed, J. Appl. Polym. Sci. 92 (2004) 2724.
[23] A.M. Alb, E. Mignard, M.F. Drenski, W.F. Reed, Macromol. 37 (2004) 2578.
[24] G.A. Sorci, W.F. Reed, Langmuir 18 (2002) 353.
[25] G.A. Sorci, W.F. Reed, Macromol. 35 (2002) 5218.
[26] D.P. Norwood, W.F. Reed, Int. J. Polym. Ana. Charact. 4 (1999) 99.
[27] R.D.C. Michel, W.F. Reed, Biopolym. 53 (2000) 19.
[28] Malabar, Fl. B.J. Berne, R. Pecora, *Dynamic Light Scattering*, 1990.
[29] A. Striegel (Ed.), Multiple Detection in Size Exclusion Chromatography, vol. 893, ACS, 2004.
[30] Part 1, ch. 12. L.D. Landau, E.M. Lifschitz, Statistical Physics, 3rd Ed, Pergamon Press, Oxford, 1963.
[31] C.E. Reed, W.F. Reed, J. Chem. Physics 94 (1991) 8479.
[32] P.J. Flory, T.G. Fox, J. Am. Chem. Soc. 73 (1951) 1904.
[33] H. Yamakawa, Modern Theory of Polymer Solutions, Harper and Row, N.Y., 1971.
[34] G. Weill, B. des Cloizeaux, J. Physique (France) 40 (1979) 99.
[35] T. Odijk, Biopolymers 18 (1979) 3111.